Satellite-Based Energy Balance to Assess Within-Population Variance of Crop Coefficient Curves

Masahiro Tasumi[1]; Richard G. Allen[2]; Ricardo Trezza[3]; and James L. Wright[4]

Abstract: Quantifying evapotranspiration (ET) from agricultural fields is important for field water management, water resources planning, and water regulation. Traditionally, ET from agricultural fields has been estimated by multiplying the weather-based reference ET by crop coefficients (K_c) determined according to the crop type and the crop growth stage. Recent development of satellite remote sensing ET models has enabled us to estimate ET and K_c for large populations of fields. This study evaluated the distribution of K_c over space and time for a large number of individual fields by crop type using ET maps created by a satellite based energy balance (EB) model. Variation of K_c curves was found to be substantially larger than that for the normalized difference vegetation index because of the impacts of random wetting events on K_c, especially during initial and development growth stages. Two traditional K_c curves that are widely used in Idaho for crop management and water rights regulation were compared against the satellite-derived K_c curves. Simple adjustment of the traditional K_c curves by shifting dates for emergence, effective full cover, and termination enabled the traditional curves to better fit K_c curves as determined by the EB model. Applicability of the presented techniques in humid regions having higher chances of cloudy dates was discussed.

DOI: 10.1061/(ASCE)0733-9437(2005)131:1(94)

CE Database subject headings: Evapotranspiration; Satellites; Remote sensing; Irrigation scheduling; Water resources management; Crops.

Introduction

For more than 30 years, the primary method for estimating evapotranspiration (ET) has been from reference ET and crop coefficient (K_c) curves (Jensen 1973; Allen et al. 1998). Crop coefficients generally found in literature, such as by Doorenbos and Pruitt (1977), Wright (1981, 1982, and 1995), Snyder et al. (1989a, 1989b), Jensen et al. (1990), and Allen et al. (1998), represent average to optimum agricultural management under well-watered conditions. These coefficients are typically determined from point-based measurements, and are unable to describe the variation in K_c for the large population of fields in a region because "mean" K_c curves must represent a single averaged crop growth and water management condition. Actual K_c populations have inherent variation because of variation in crop variety, irrigation method, weather, soil type, salinity and fertility, and/or field management that can be different from the field used to establish the literature values. This is especially true under water limiting or extreme salinity conditions. Quantification and characterization of K_c populations for various crops in a region would be valuable in defining average water use by crop type under field conditions and the range in water use. This type of information can be helpful in determining impacts of water scarcity or need for remedial help in improving water or agronomic management.

Alternative means for estimating field-scale ET include satellite image-based remote sensing methods. These methods might be divided into two categories: empirical/statistical approaches and energy balance (EB) approaches. Empirical/statistical approaches correlate ET either to air–surface temperature differences such as reported by Caselles et al. (1998), or to vegetation indices as frequently used for "basal" K_c estimation for agricultural crops (Neale et al. 1989; Choudhury et al. 1994; Hunsaker et al. 2003). On the other hand, EB approaches derive ET through completing a full energy balance computation using methods such as a two-layer model and the dual-temperature-difference method developed by Norman et al. (1995 and 2000), surface energy balance algorithms for land (SEBAL) model (Bastiaanssen et al. 1998a), and evaporation fraction estimation method for *MODIS* (Nishida et al. 2003). In this study, a satellite-based EB model, which is a variant of the SEBAL model, was applied to determine actual K_c for a large number of agricultural fields in southern Idaho. Crop coefficients derived from the EB model are compared to widely used K_c curves in Idaho, and the potential and applicability of satellite based K_c curves are discussed.

Energy Balance Model

The SEBAL is an ET estimation approach based on satellite images via the computation of a land surface energy balance meth-

[1]Post-Doctoral Researcher, Univ. of Idaho Research and Extension Center, 3793 N. 3600 E., Kimberly, ID 83341. E-mail: tasumi@kimberly.uidaho.edu

[2]Professor, Water Resources Engineering, Univ. of Idaho Research and Extension Center, 3793 N. 3600 E., Kimberly, ID 83341. E-mail: rallen@kimberly.uidaho.edu

[3]Associate Professor, Univ. of the Andes, Merida, Venezuela.

[4]Soil Scientist, USDA-ARS Northwest Irrigation and Soils Research Laboratory, 3793 N. 3600 E., Kimberly, ID 83341.

Note. Discussion open until July 1, 2005. Separate discussions must be submitted for individual papers. To extend the closing date by one month, a written request must be filed with the ASCE Managing Editor. The manuscript for this paper was submitted for review and possible publication on May 6, 2003; approved on January 8, 2004. This paper is part of the ***Journal of Irrigation and Drainage Engineering***, Vol. 131, No. 1, February 1, 2005. ©ASCE, ISSN 0733-9437/2005/1-94–109/ $25.00.

odology developed by Bastiaanssen (Bastiaanssen et al. 1998a; Bastiaanssen 2000). The model has been tested at a number of locations especially in arid–semiarid regions including Spain, Italy, Turkey, Pakistan, India, Sri Lanka, Egypt, Niger, and China (Bastiaanssen et al. 1998b; Bastiaanssen and Bos 1999; Hemakumara et al. 2003; 2005). The EB model used in this study is a variant of the SEBAL model of Bastiaanssen (Bastiaanssen et al. 1998a), extended by the Univ. of Idaho (Tasumi et al. 2000, 2003; Allen et al. 2002, 2003) for applications in the western United States, where generally good networks of electronic agricultural weather stations are available. The two major extensions to SEBAL are: (1) modifying the internal procedure to calibrate the energy at the two extreme conditions (i.e., wet and dry conditions) utilizing reference ET as predicted by the ASCE standardized Penman–Monteith alfalfa-reference ET procedure (EWRI 2002) for the wet condition, and a surface soil layer water balance based on the *FAO-56* soil evaporation estimation procedure (Allen et al. 1998) for the dry condition, and (2) incorporating relatively complex geometric equations to integrate solar radiation incident to sloping terrain over 24 h periods. The first extension refines the accuracy for predicting ET from agricultural crops by calibrating the latent heat flux density at the two extreme conditions, and it makes the EB model consistent with the reference crop ET approach. This style of internal calibration eliminates the need for external atmospheric correction for surface albedo and temperature estimation, because the linear calibration function for sensible heat estimation in the energy balance does not carry constant or linear types of error generated during intermediate calculations into the ET estimate (Tasumi et al. 2003). Use of ET_r during image processing fosters congruency between K_c values determined from the EB model and traditional ground-based K_c methods. It also facilitates extrapolation of crop ET between image dates using intervening weather data (Allen et al. 2002). The second extension provided for application of the EB model to mountainous regions using a digital elevation model (DEM). The EB model has been tested (Allen et al. 2002; Tasumi et al. 2003) and applied in Idaho (Morse et al. 2000, 2001; Allen et al. 2003). A later section provides a comparison of the EB model with lysimeter measurements of ET.

In the EB model, ET is estimated as the residual of an energy balance applied to the land surface for each pixel of the satellite image (e.g., for each 30 m × 30 m square for Landsat 5 TM and Landsat 7 ETM+ images)

$$\lambda E = R_n - H - G \tag{1}$$

where λE = latent heat flux (W m^{-2}); R_n = net radiation (W m^{-2}); H = sensible heat flux (W m^{-2}); and G = soil heat flux (W m^{-2}).

Net radiation is computed from the land surface radiation balance as

$$R_n = (1 - \alpha)R_s + (\varepsilon L_{\text{in}} - L_{\text{out}}) \tag{2}$$

where α = surface albedo; R_s = solar radiation (W m^{-2}); ε = surface emissivity for accounting for reflectance of incoming longwave radiation at land surface; and L_{in} and L_{out} = incoming and outgoing longwave radiation (W m^{-2}), respectively. Surface albedo is determined by integrating at-satellite spectral reflectances in the six short-wave bands of the Landsat image and then applying a correction based on general air transmittance estimated using elevation and humidity (EWRI 2002). L_{in} is calculated using air temperature as approximated from satellite-derived surface temperature for a wet agricultural field and using a regionally calibrated air emissivity. L_{out} is computed as a function of surface temperature derived from the satellite image. Surface emissivity is computed from vegetation indices derived from two of the short-wave bands. Potential values for R_s are determined using theoretical clear sky curves (Allen 1996; EWRI 2002).

The normalized difference vegetation index (NDVI) in the EB model is calculated using at-satellite reflectances of Bands 3 and 4 of Landsat

$$\text{NDVI} = \frac{\text{ref}_4 - \text{ref}_3}{\text{ref}_4 + \text{ref}_3} \tag{3}$$

where ref_3 and ref_4 = at-satellite reflectances for Bands 3 and 4, respectively.

Soil heat flux is empirically estimated using a function by Bastiaanssen (2000) based on albedo, surface temperature, NDVI, and net radiation

$$G = (T_s - 273.16)(0.0038 + 0.0074\alpha) \times (1 - 0.98\text{NDVI}^4)R_n \tag{4}$$

where T_s = surface temperature in Kelvin.

Sensible heat flux in the EB model is estimated from wind speed and surface temperature using an "internally calibrated" near surface to air temperature difference function, similar to SEBAL (Bastiaanssen et al. 1998a; Bastiaanssen 2000)

$$H = \frac{\rho_{\text{air}} C_p (a + bT_s)}{r_{\text{ah}}} \tag{5}$$

where ρ_{air} = air density(kg m^{-3}); C_p = specific heat capacity of air ($\approx$1,004 J kg^{-1} K^{-1}); r_{ah} = aerodynamic resistance to heat transport (s m^{-1}); T_s = surface temperature (K); and a and b = empirical coefficients determined through the internal calibration for each satellite image. The term "$a + bT_s$" in the equation represents the near surface to air temperature difference dT predicted between a height near the surface (0.1 m) and a height at about 2 m above the surface. Use of an internally calibrated dT (i.e., gradient) largely compensates for problems caused by differences between radiometric and aerodynamic surface temperature and the unknown spatial variation in air temperature as, for example, described by Moran et al. (1989) and Kustas and Norman (1996). Determination of r_{ah} in Eq. (5) requires iteration for air stability corrections applying Monin–Obukhov similarity theory (Bastiaanssen 2000).

The internal calibration of the EB model trains the surface energy balance to predict ET for the two extreme conditions referred to as "cold" and "hot" pixels resembling full-cover, well-watered alfalfa and a dry agricultural bare soil, respectively. The ET values for these two conditions are estimated by weather data, assisted by the ASCE standardized Penman–Monteith alfalfa-reference ET procedure (EWRI 2002) and an *FAO-56* based water balance applied to the surface soil layer (Allen et al. 1998). Values for dT at these two extreme pixels are back calculated based on the energy balance, and the empirical coefficients a and b in Eq. (5) are determined assuming a linear relation between dT and surface temperature. When systematic errors in intermediate calculations (e.g., albedo, surface temperature, net radiation, and soil heat flux) occur, the internal calibration process compensates the intermediate errors by deriving a "biased" dT function. This makes the ET estimate consistent with the expected ET as predicted by weather data and satellite image data at the two extreme conditions. In contrast to the EB model, SEBAL (Bastiaanssen et al. 1998a) typically uses T_s from a local water body as the cold pixel, and defines H and dT for the pixel as zero. The SEBAL defines ET from the hot pixel is zero. The simpler definitions for the two extreme pixels in SEBAL makes the model applicable for

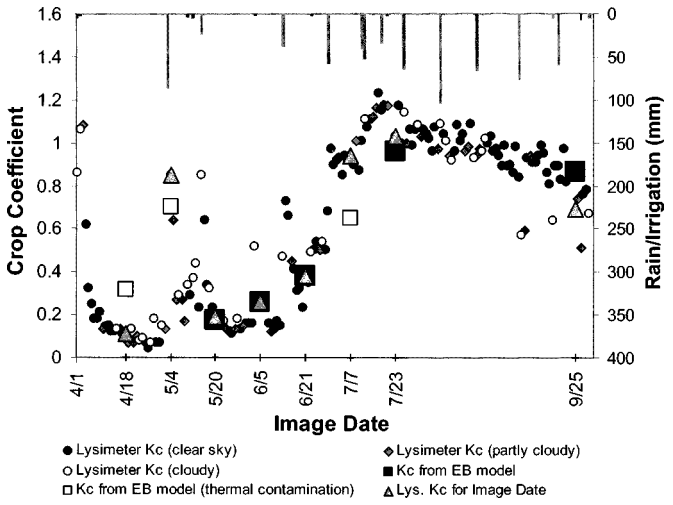

Fig. 1. Comparison of K_c by energy balance model and by lysimeter for sugar beets near Kimberly, Id., 1989 (unpublished lysimeter data from Wright, 2000, USDA-ARS, Kimberly, Id.). Cloud levels were defined by ratio of measured solar radiation to theoretical clear sky solar radiation (R_s/R_{so}) as; "clear sky:" $R_s/R_{so} \geq 0.85$; "partly cloudy:" $0.7 \leq R_s/R_{so} < 0.85$; "cloudy:" $R_s/R_{so} < 0.7$.

countries where high-quality weather data are difficult to obtain. However, the practice of assuming $H=0$ at water body temperature may cause some error in the estimate of H and ET for cold agriculture pixels in arid regions (Tasumi 2003).

Once ET at the moment of the satellite image is estimated, the crop coefficient (K_c) is calculated for each image pixel as

$$K_c = \frac{\mathrm{ET}}{\mathrm{ET}_r} \tag{6}$$

where ET_r = alfalfa reference ET calculated from local weather data using the ASCE standardized Penman–Monteith alfalfa reference method (EWRI 2002) applied hourly.

For horizontal flat surfaces, 24 h ET is estimated by setting the 24 h average K_c equal to the "instantaneous" K_c calculated in Eq. (6)

$$\mathrm{ET}_{(24)} = K_c \mathrm{ET}_{r(24)} \tag{7}$$

The K_c in Eqs. (6) and (7) has also been referred to as the ET_r fraction ($\mathrm{ET}_r\mathrm{F}$) (Allen et al. 2002, 2003), and has been shown to be relatively consistent during daytime periods and between 24 h average and midday satellite image times (Allen et al. 2002; Trezza 2002; Tasumi 2003; Romero 2003). Additional adjustments are applied during the extrapolation of K_c from instantaneous to 24 h for sloping surfaces. Monthly and seasonal K_c and ET can further be estimated by linearly interpolating the K_c values over periods inbetween two consecutive images.

Sample Comparison of Evapotranspiration and K_c Predictions with Lysimeter Measurements

Crop coefficients and the cumulative ET derived from the satellite based EB model are compared with independent lysimeter-measured data from the USDA-ARS facility at Kimberly, Id. (Wright 1982) for a sugar beet crop grown in 1989 (Figs. 1 and 2). The lysimeter data were measured by a 1.8×1.8 m weighing lysimeter having resolution of about 0.07 mm for daily readings (Wright 1991). Nine Landsat images from April to September

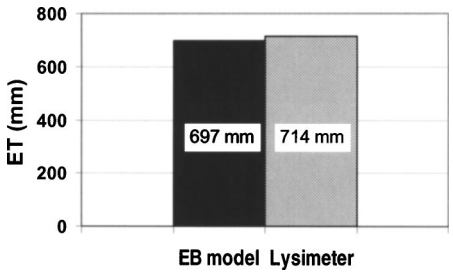

Fig. 2. Seasonal evapotranspiration (April–September 1989) by energy balance model and lysimeter measurement for sugar beets near Kimberly, Id. (unpublished lysimeter data from Wright 2000, USDA-ARS, Kimberly, Id.)

1989 were used for the comparison. No cloud-free Landsat images were available during August–early September. The 180×140 m lysimeter research field was smaller than the minimum requirement of 240×240 m that would ensure at least one 120×120 m thermal pixel of Landsat 5 to reside completely inside the field for all images. For this reason, the satellite observed surface temperatures for pixels over the lysimeter field were occasionally impacted by portions of pixels lying over adjacent plots having dissimilar field conditions and temperature. Evapotranspiration is not estimated with typical accuracy when the thermal pixel over the lysimeter is heavily contaminated by areas outside of the lysimeter field because the EB model relies heavily on the thermal band information to solve the energy balance. Estimated K_c for dates having heavy thermal contamination problems could not be used for evaluating model accuracy. Results for these dates are labeled "K_c from EB model (thermal contamination)" in Fig. 1. This type of thermal contamination is not a problem for larger fields (>10 ha), except for about 50 m (Landsat 7) to 100 m (Landsat 5) strips around the field boundaries.

The predicted K_c by the EB model agreed well with the lysimeter measured values throughout the course of the growing season as the sugar beet field progressed from bare soil to full cover. Overall, the absolute difference between the EB model and lysimeter-derived K_c values averaged 0.05 with the exclusion of the three heavily contaminated dates for the thermal band pixel as noted previously. This is considered to be good predictive accuracy. The difference in estimated and lysimeter measured seasonal ET (April–September 1989) was only 17 mm (Fig. 2), because ET prediction errors for each image date behaved in a random manner and thus provided compensation while integrating over time. Bastiaanssen et al. (2005) provide a summary of error and uncertainty in ET estimates by SEBAL.

Methodology

The study area is an agricultural area in south central Idaho known locally as Magic Valley (Fig. 3). Magic Valley has a semi-arid climate with annual precipitation of 280 mm (30 year average). The agriculture relies on irrigation from the Snake River and regional groundwater systems. Center pivot, wheel line, and furrow irrigation are the predominant irrigation systems in the area. The major crops are alfalfa, beans, corn, pasture, potatoes, sugar beets, winter and spring small grains, and peas.

Data input for the EB model included Landsat satellite images, a DEM, a landuse map, and hourly weather data. In this study, 12 Landsat satellite images (path40/row30) acquired March–October

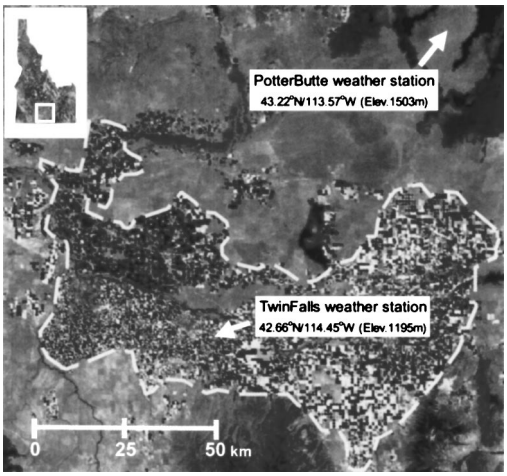

Fig. 3. Magic Valley agricultural study area (circled by dotted line) and locations of weather stations

2000 by either Landsat 5 or 7 satellite were processed. Images (either Landsat 5 or 7) were available as frequently as every 8 days, depending on cloud conditions. The 12 image dates selected are March 15, April 8, March 2, June 3, June 19, July 5, July 21, August 14, August 22, September 7, September 15, and October 17, 2000. The Landsat overpass time was approximately 10:56 to 11:10 a.m. local standard time. A landuse map for the corresponding area was derived from the same satellite images and was used to predict aerodynamic roughness for the terrain. Weather data were obtained from the Twin Falls AgriMet weather station (U.S. Bureau of Reclamation), representative of agriculture areas, and from the Potter Butte RAWS weather station (U.S. Bureau of Land Management), representative of deserts surrounding the study area (Fig. 3). The ET_r was computed as a weighted average of the two stations with 80% weight given to the Twin Falls station, determined by considering the locations and landuses surrounding the two weather stations. All weather data were subjected to quality control analyses as described in EWRI (2002). Using the satellite image with ground truth information, a crop type classification map for the Magic Valley agricultural areas were derived for use in the K_c curve analysis. By the classification, about 70% of the agricultural area in the Magic Valley study area encircled by the dotted line in Fig. 3 was classified into one of the following eight crop groups: alfalfa, beans, sugar beets, corn, peas, potatoes, spring grain, and winter grain. About 20% of the classified fields were omitted from the analysis because of small field size that prevented sampling of interior pixels.

Crop coefficients (K_c) for the 12 image dates were computed from the ET maps determined by the EB model on a pixel by pixel basis. The Landsat images have spatial resolution of 30 by 30 m for the shortwave bands, and 60 m (Landsat 7 ETM+) or 120 m (Landsat 5 TM) for the thermal infrared band. The resolution of calculated K_c maps are thus 60 or 120 m, as the EB model relies on the thermal band information to solve the energy balance. Theoretically, a minimum field size of 240×240 m is required to ensure that at least one 120 m thermal pixel exists that is purely from the field area. The typical field sizes in the study area are on the order of 400×400 m-800×800 m. Therefore, the resolutions of the Landsat based ET images are fine enough to permit quantification of ET from most individual agricultural fields by sampling interiors of fields. Minor fields having sizes less than 400×400 m were rejected and were not used for the analysis. For all remaining fields, one sample pixel internal to the field was selected, and K_c and NDVI values were retrieved for the analyses.

Finally, K_c curves derived by the EB model for the eight major crop types were compared to widely used K_c curves in Idaho by Allen and Brockway (1983) and by AgriMet (2002b). The Allen and Brockway K_c curves were based on planting, full cover and harvest dates for various subregions of Idaho representing long-term averages, and used K_c curves developed by Wright (1981). The K_c values were summarized in that report as monthly averages. The AgriMet K_c curves are also based on Wright (1981) K_c tables with later refinements by Wright (1995) and by the U.S. Bureau of Reclamation (AgriMet 2002a), with modification by the Bureau of Reclamation to express the K_c curve for the total growing period as a function of percentage from emergence to effective full cover and percentage of effective full cover to termination (i.e., harvest).

Results and Discussion

Characteristics of K_c and Vegetation Indices for 3,888 Classified Fields

The distribution of the K_c derived by the EB model and the corresponding NDVI values are shown in Figs. 4 and 5 for all classified fields for all 12 image dates. The variation in K_c among fields by date was generally greater than that for NDVI due to the impact of soil wetness on individual values for K_c. The NDVI is largely unaffected by soil moisture. During periods of full cover, the variation in K_c reduced because of the tendency for transpiration from crops to consume most of the available energy, thereby leaving less energy for direct evaporation of soil water. The periods of highest variation in K_c were during the development periods and periods of senescence or postharvest where NDVI was less than 0.6 (Figs. 4 and 5). Sample means and standard deviations for K_c and NDVI are summarized in Tables 1 and 2 for the eight crop categories and 12 image dates.

In general, the standard deviations for K_c populations averaged about 0.25 during periods of largest variation (periods of crop development and senescence) and about 0.09 during peak periods. Corresponding values for the coefficient of variation (standard deviation divided by the mean) averaged about 0.5–0.7 during the periods of large variation and about 0.1 during peak periods.

Many of the K_c and NDVI distributions approximated normal distributions and had little skew, especially when sample variance was small. As sample variance increased, for example during crop development, some skewness was evident. The positive skews in the K_c populations during development period reflect those fields experiencing substantial evaporation due to recent wetting by irrigation. Negative skews during full cover reflect the upper limit on ET imposed by energy availability. The averages for K_c and NDVI by date are plotted on the graphs in Figs. 4 and 5. The more symmetrical samples are discernable as those where the averaged value overlies the peak of the sample distribution (modal value). During the crop development and senescing periods, K_c is strongly impacted by the irrigation practices of individual fields. Also shifts in the planting schedules among fields appear as a wide range of K_c during the crop development and the harvest periods where the crop condition can dramatically change within a short time. The variation in K_c caused by differences in planting schedule is directly linked to variation in NDVI. Therefore, one might further investigate the "bandwidth" of K_c for the

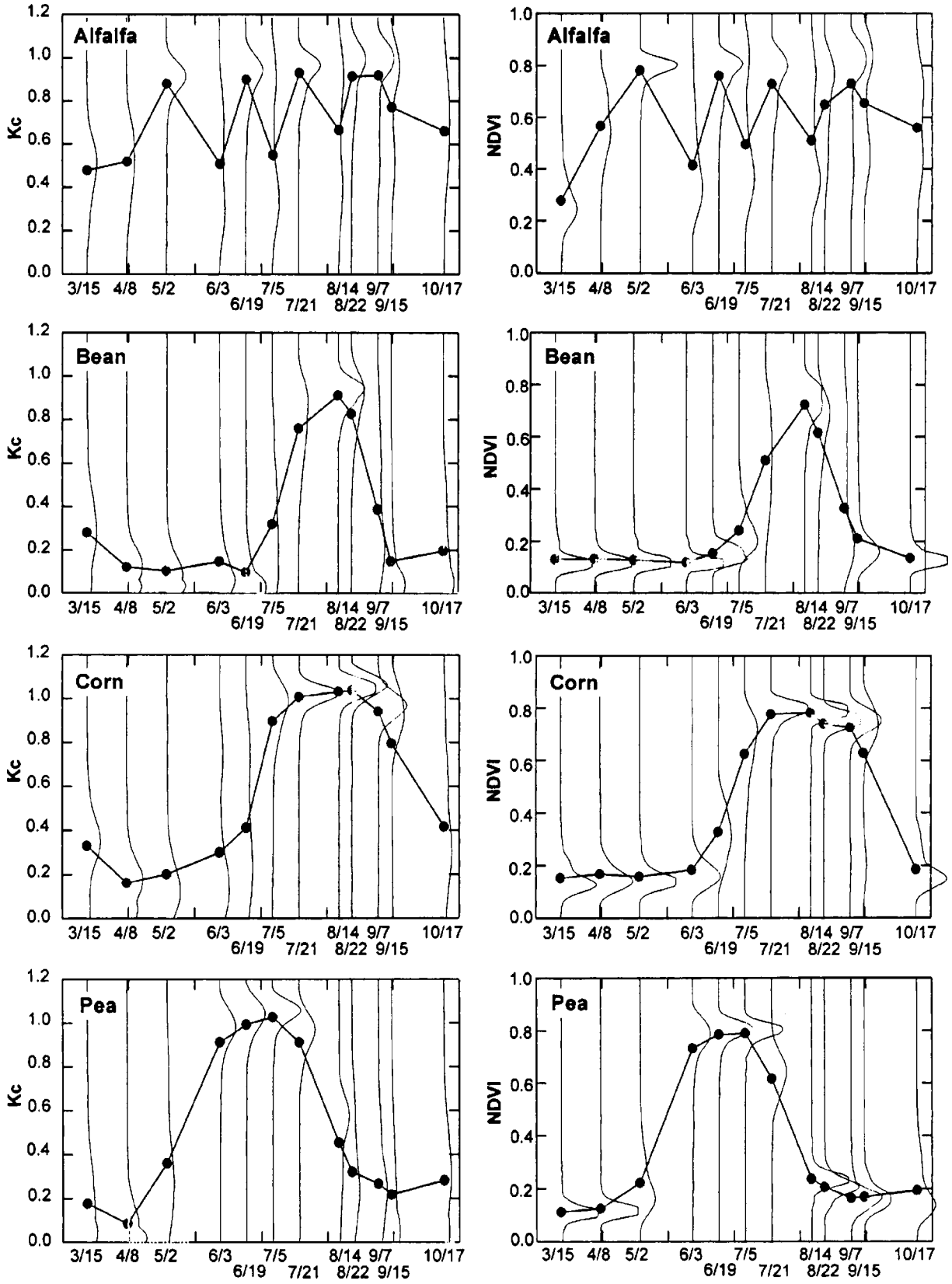

Fig. 4. Distribution of K_c and normalized difference vegetation index for all classified fields in study area for 2000

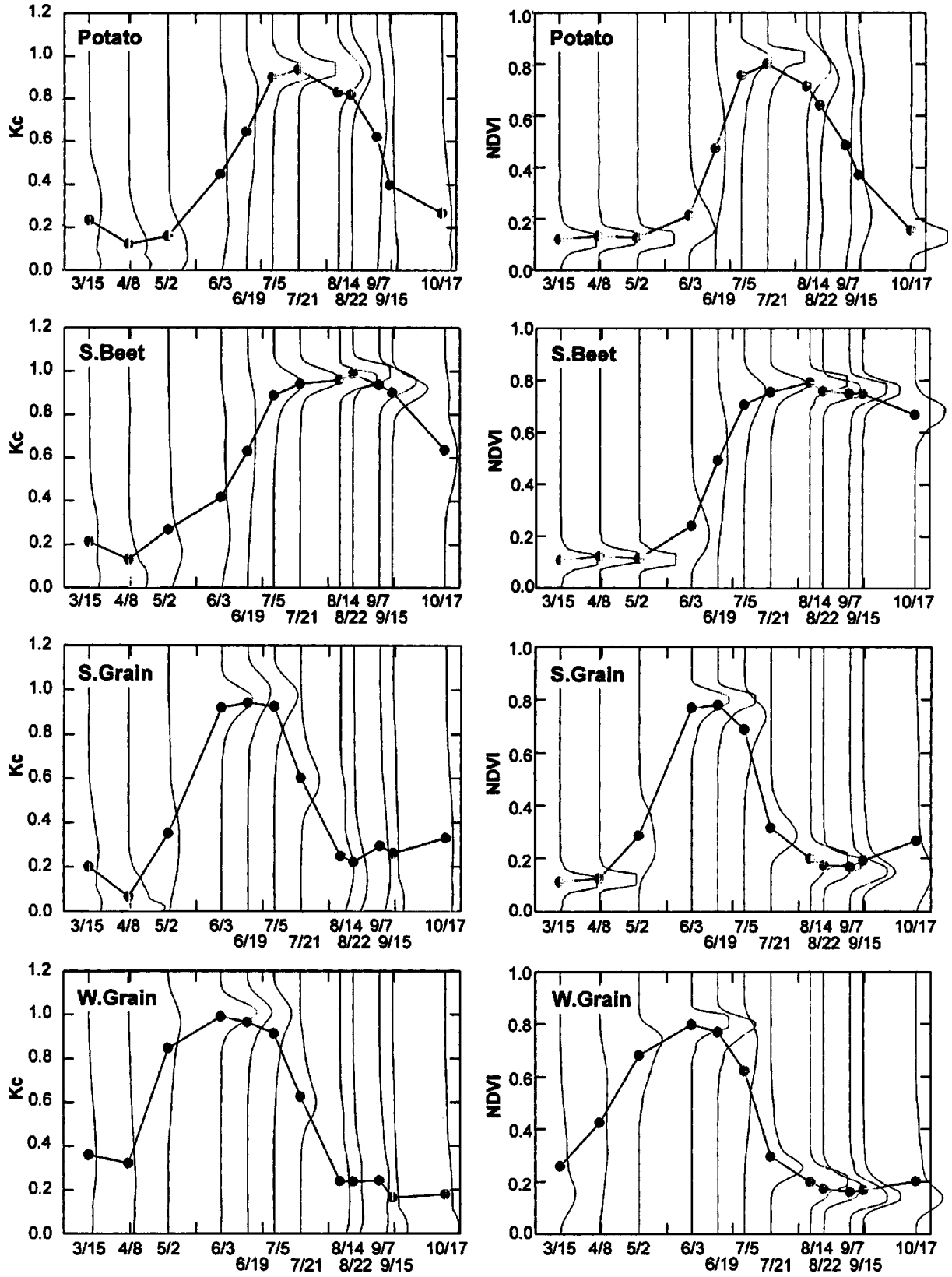

Fig. 5. Distribution of K_c and normalized difference vegetation index for all classified fields in study area for 2000

Table 1. Means and Standard Deviations of Crop Coefficient (K_c) Values Derived by Satellite Based Energy Balance for 3,888 Classified Fields in Magic Valley during 2000

Statistics	Image date	Alfalfa	Bean	Corn	Pea	Potato	Sugar beet	Spring grain	Winter grain
Mean	3/15/00	0.48	0.28	0.33	0.18	0.23	0.21	0.20	0.36
	4/8/00	0.52	0.12	0.16	0.08	0.12	0.13	0.07	0.32
	5/2/00	0.88	0.10	0.20	0.36	0.16	0.27	0.35	0.85
	6/3/00	0.51	0.15	0.30	0.91	0.45	0.42	0.92	0.99
	6/19/00	0.90	0.10	0.41	0.99	0.65	0.63	0.94	0.96
	7/5/00	0.55	0.32	0.90	1.03	0.90	0.89	0.93	0.91
	7/21/00	0.93	0.76	1.01	0.91	0.94	0.94	0.60	0.63
	8/14/00	0.67	0.91	1.03	0.45	0.83	0.96	0.25	0.24
	8/22/00	0.91	0.83	1.04	0.32	0.82	0.99	0.22	0.24
	9/7/00	0.92	0.39	0.94	0.27	0.62	0.94	0.29	0.24
	9/15/00	0.77	0.15	0.79	0.22	0.40	0.90	0.26	0.16
	10/17/00	0.66	0.20	0.42	0.28	0.27	0.64	0.33	0.18
Standard deviation	3/15/00	0.15	0.17	0.16	0.16	0.17	0.19	0.17	0.22
	4/8/00	0.17	0.10	0.11	0.11	0.13	0.21	0.09	0.25
	5/2/00	0.14	0.10	0.19	0.23	0.17	0.21	0.20	0.18
	6/3/00	0.23	0.17	0.27	0.17	0.25	0.23	0.09	0.09
	6/19/00	0.12	0.16	0.27	0.14	0.20	0.21	0.11	0.12
	7/5/00	0.27	0.23	0.18	0.10	0.08	0.11	0.11	0.16
	7/21/00	0.10	0.17	0.06	0.16	0.04	0.10	0.13	0.15
	8/14/00	0.28	0.07	0.06	0.18	0.21	0.03	0.17	0.17
	8/22/00	0.16	0.18	0.11	0.20	0.24	0.05	0.18	0.18
	9/7/00	0.18	0.25	0.12	0.18	0.25	0.07	0.21	0.18
	9/15/00	0.25	0.21	0.29	0.22	0.34	0.07	0.25	0.21
	10/17/00	0.24	0.20	0.25	0.19	0.22	0.16	0.25	0.19
Number of classified fields[a]		325	432	474	314	717	516	546	564

[a]Classified fields include only fields having size of 400 m by 400 m or larger.

same growing stage of a crop by eliminating differences in the planting schedule through shifting K_c curves from each field to make the peaks of the NDVI curves for all fields the same. In this study, the variance in K_c caused by differences in planting schedules was retained in order to capture the overall average and variance for actual field management and cultural conditions in the study area.

Maximum values for K_c for individual fields peaked at about 1.10 for alfalfa, corn, peas, spring grain, and winter grain, and about 1.05 for beans, potatoes, and sugar beets (Figs. 4 and 5). Modal values for K_c (defined as the value of the 0.01 increment having the highest occurrence) during periods of full cover were close to 1.0 for alfalfa, spring grain, and winter grain, and averaged 1.04, 1.02, 0.95, 0.94, and 0.97 for corn, peas, bean, potatoes, and sugar beets (Table 3). These modal values, representing the most frequently occurring value, characterize the typical K_c value for fields at full cover for the image dates when NDVI was at its maximum or near maximum value. Table 3 compares these modal values with the maximum K_c value recommended by Wright (1981) for the same crops. The modal values are quite similar to the peak values of Wright (1981) except for potatoes, where Wright's value of 0.78 is much less than the average modal value of 0.94. Some of this difference may be caused by differences in modern varieties of potatoes and planting densities and in impacts of differences between irrigation system types, with center pivot irrigation being practiced on most potatoes in Magic Valley during 2000 as compared to less frequent solid-set sprinkler irrigation practiced during the measurements by Wright (1981). It is noted that K_c values derived by Wright (1981) were based on the 1982 Kimberly Penman alfalfa reference method (Wright 1982) computed daily, whereas the EB model derived K_cs were based on the standardized Penman–Monteith alfalfa reference method computed hourly. Small differences between the two methods have been evaluated and summarized by EWRI (2002). However, because the same ET_r method was used in the EB model calibration and to determine K_cs from the sampled fields, the K_c values obtained from the EB model were not biased by the reference ET method and are thus directly comparable to those by Wright (1981).

Some of the extreme K_c values for individual fields (those greater than 1.05) were no doubt caused by estimation error of the EB model or may be due to differences in weather conditions within the 120 by 70 km study area. The EB model assumes that the weather condition of entire study area is the same when computing crop coefficients. This error range has been observed to change with image size and thus variation in weather conditions of the study area. For the study area described here, the K_c estimation error caused by the differences in weather conditions across the area is probably less than ±0.05, which is an acceptable range of error. Values for K_c that fall in the range of 1.0–1.05 may represent fields that were recently irrigated so that the canopy surface is wet or where the canopy may have dried, but the soil

Table 2. Means and Standard Deviations of Normalized Difference Vegetation Index for 3,888 Classified Fields in Magic Valley during 2000

Statistics	Image date	Alfalfa	Bean	Corn	Pea	Potato	Sugar beet	Spring grain	Winter grain
Mean	3/15/00	0.28	0.13	0.15	0.11	0.12	0.11	0.11	0.26
	4/8/00	0.57	0.13	0.17	0.12	0.13	0.12	0.12	0.42
	5/2/00	0.78	0.13	0.16	0.22	0.13	0.11	0.29	0.68
	6/3/00	0.41	0.12	0.18	0.73	0.21	0.24	0.77	0.80
	6/19/00	0.76	0.15	0.33	0.79	0.47	0.49	0.78	0.77
	7/5/00	0.49	0.24	0.62	0.79	0.76	0.71	0.69	0.62
	7/21/00	0.73	0.51	0.78	0.62	0.80	0.75	0.32	0.30
	8/14/00	0.51	0.72	0.78	0.24	0.72	0.79	0.20	0.20
	8/22/00	0.65	0.62	0.74	0.21	0.64	0.76	0.18	0.17
	9/7/00	0.73	0.33	0.72	0.16	0.49	0.75	0.17	0.16
	9/15/00	0.65	0.21	0.63	0.17	0.37	0.75	0.19	0.17
	10/17/00	0.56	0.14	0.18	0.19	0.16	0.67	0.27	0.20
Standard deviation	3/15/00	0.09	0.06	0.06	0.04	0.05	0.03	0.04	0.14
	4/8/00	0.11	0.06	0.07	0.04	0.05	0.02	0.03	0.17
	5/2/00	0.06	0.04	0.05	0.09	0.03	0.03	0.10	0.08
	6/3/00	0.15	0.02	0.09	0.13	0.08	0.09	0.06	0.03
	6/19/00	0.07	0.03	0.11	0.07	0.15	0.14	0.05	0.05
	7/5/00	0.20	0.07	0.13	0.04	0.10	0.09	0.09	0.14
	7/21/00	0.11	0.16	0.06	0.09	0.05	0.08	0.08	0.09
	8/14/00	0.19	0.07	0.04	0.04	0.18	0.03	0.04	0.04
	8/22/00	0.15	0.13	0.07	0.04	0.19	0.03	0.04	0.04
	9/7/00	0.17	0.21	0.12	0.05	0.22	0.05	0.06	0.05
	9/15/00	0.19	0.12	0.21	0.05	0.22	0.05	0.09	0.06
	10/17/00	0.17	0.03	0.07	0.09	0.10	0.05	0.19	0.11
Number of classified fields[a]		325	432	474	314	717	516	546	564

[a]Classified fields include only fields having size of 400 m by 400 m or larger.

surface is very wet. Under these conditions, the K_c is expected to exceed 1.0 representing the alfalfa reference. This is especially true for crops like corn that have larger aerodynamic roughness than alfalfa.

Peak values for the estimated K_c averaged over all fields are included in Table 3. These values are generally lower than modal values due to impacts of some fields having relatively low NDVI. Averages of the estimated peak values were greater than peak values of Wright (1981) for three crops (corn, peas, and potatoes), essentially equal to Wright (1981) for two crops (sugar beets and winter grain), and lower than Wright (1981) for two crops (beans and spring grain). The lower average peak K_c for spring grain may have been partly caused by a wide range in planting dates, causing individual fields to reach full cover and then begin to senesce at different times. Alfalfa K_c values from the EB model were not compared with peak values of Wright (1981) because of the lowering of average K_c for all image dates, caused by the occurrence of some recently harvested fields being in less than full cover condition on each image date. In general, agreement between the estimated peak K_c and Wright (1981) is considered to be very good. The following sections are a discussion of some individual crop types regarding Figs. 4 and 5.

Table 3. Modal and Peak Mean Values for K_c Derived from Satellite Based Evapotranspiration Maps and Peak Mean K_c from Wright (1981)

Crop	Range in modal K_c from energy balance (EB) model during period of effective full cover	Peak mean K_c from EB model	Peak mean K_c from Wright (1981)
Alfalfa	0.95–1.02	n/a[a]	1.0
Bean	0.95	0.91	0.95
Corn	1.02–1.06	1.04	0.95
Pea	1.0–1.05	1.03	0.93
Potato	0.92–0.96	0.94	0.78
Sugar beet	0.95–1.0	0.99	1.0
Spring grain	0.98–1.0	0.94	1.0
Winter grain	0.98–1.02	0.99	1.0

[a]Not available.

Alfalfa

Predominately, only alfalfa fields having four-cutting cycles per year appear in Figs. 4 and 5, although a significant minority of fields in Magic Valley are cut only three times. This bias occurred because of our use of training fields during crop type classification having four cuttings. These fields represent the current trend in alfalfa management and production in the Magic Valley. The NDVI distribution shows that dates for the first cutting were relatively uniform in time among fields (Figs. 4 and 5), but became less uniform by the third and fourth cuttings, due to the integration of differences in field management and timings of cuttings.

Corn and Sugar Beets

Corn and sugar beet fields exhibited relatively consistent NDVI distributions. A relatively large variation during the crop develop-

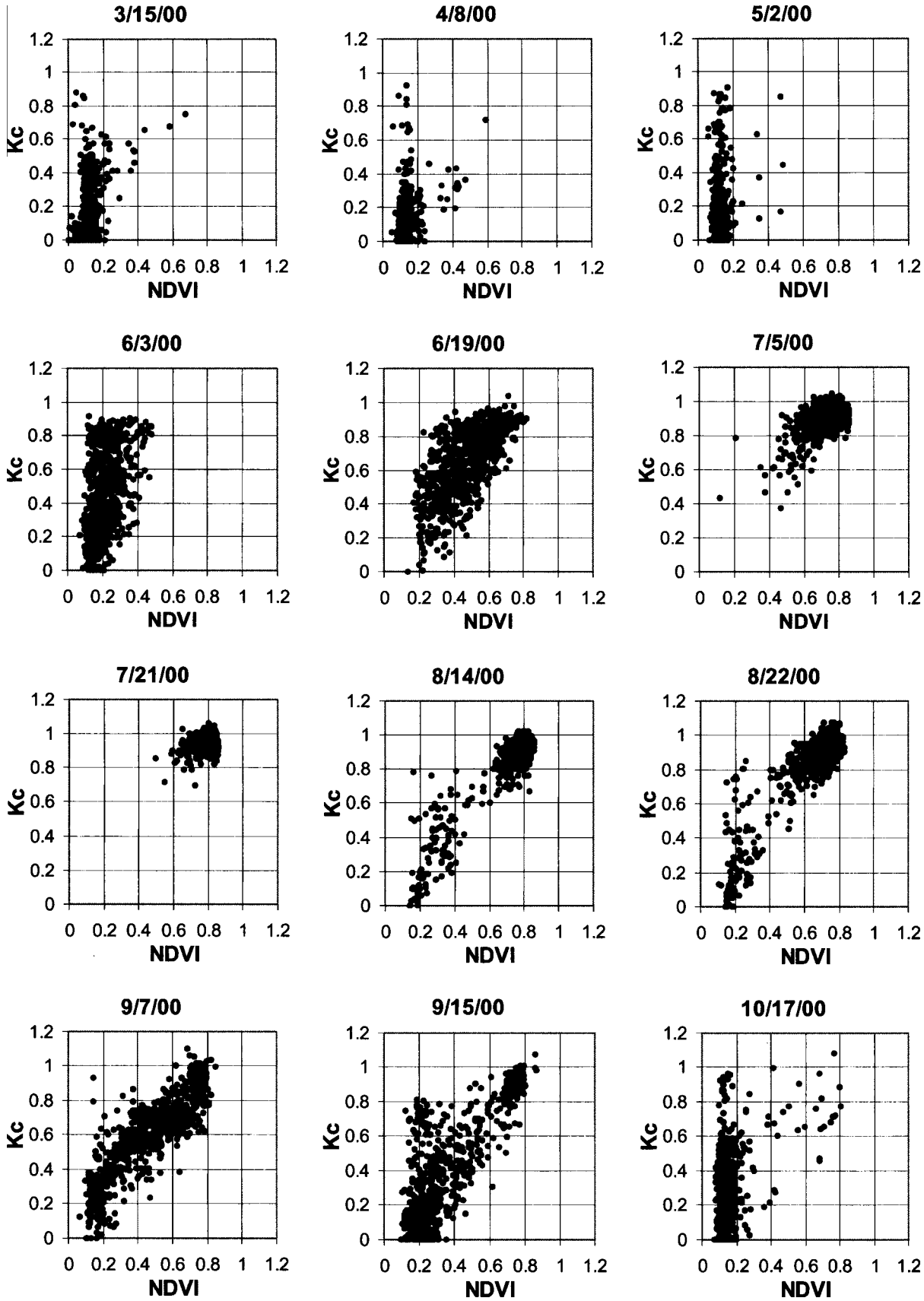

Fig. 6. K_c versus normalized difference vegetation index for 717 potato fields in study area

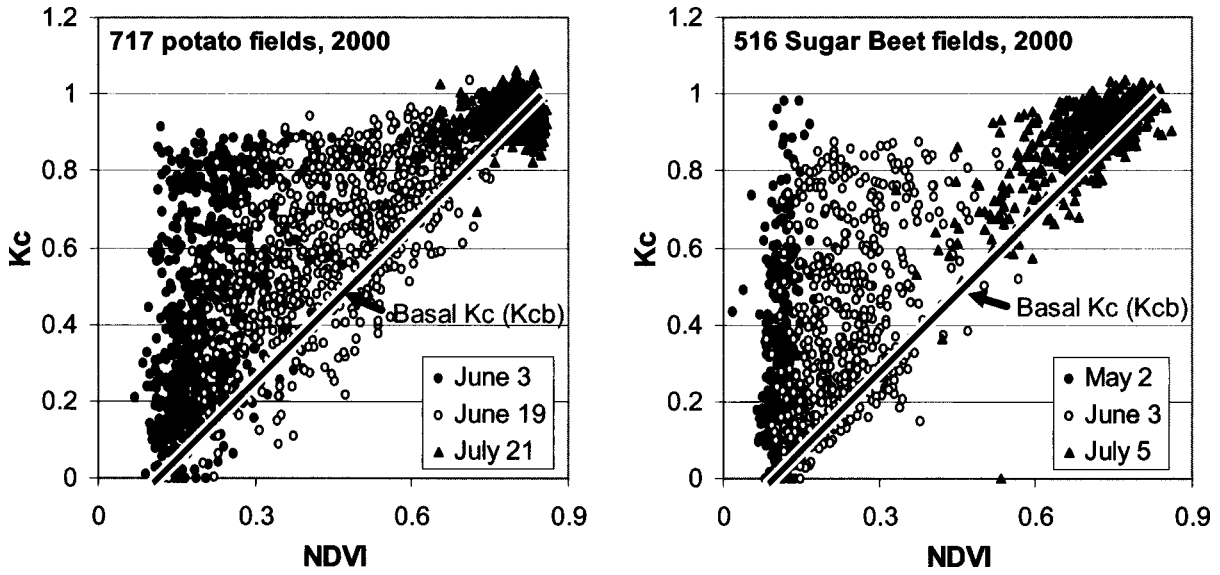

Fig. 7. Crop coefficient versus normalized difference vegetation index for 717 potato fields (left) and 516 sugar beet fields (right) in Magic Valley area of Idaho, for three Landsat dates in crop developing periods during 2000

ing periods reflects differences in crop growth among individual fields. A very large variation in K_c was exhibited during the last image date October 17. By this date, it is likely that some farmers had already terminated irrigation, causing some reduction in evaporation from soil, while others had not. In addition, much of the corn crop appears to have been harvested for silage by October 17, according to the NDVI. Therefore the wide range in K_c reflects variation in soil wetness or the presence/absence of vegetation. The relatively high NDVI on October 17 for nearly all sugar beet fields indicates that the crops were still actively growing, but with a reduced rate of transpiration, possibly due to frost or temperature effects on the stomatal opening.

Potato and Grains

Potato and grain fields had relatively wide and skewed distributions of K_c during the full cover period, while other crops showed relatively normal and symmetrical distributions for the period. This may have been caused by wider variation in the planting schedules for these crops, or the effect of two or more substantially different crop varieties. Potato crops in Magic Valley are characteristically split between early harvested varieties and late harvested varieties. Also potato growth is greatly affected by fertility and physical property of the soil. The wide range in harvesting is reflected in the wide range in NDVI during the September image dates.

Relationship between K_c and Normalized Difference Vegetation Index

Several studies and applications of remote sensing have established relationships between K_c and NDVI for purposes of mapping spatial variability in K_c (Neale et al. 1989; Bausch and Neale 1989; Bausch 1993, 1995; Choudhury et al. 1994). Most of these studies predicted primarily the transpiration coefficient or "basal" K_c, because vegetation indices are little impacted by evaporation from soil. Fig. 6 shows a series of relationships between K_c from the EB model and NDVI for potato fields throughout the year 2000. As discussed previously in Figs. 4 and 5, K_c and NDVI have a clear relation during mid season, but, as expected, no clear relation holds during periods having low ground cover due to large ranges in the soil evaporation component. Potato fields were in a bare soil condition on March 15, and therefore NDVI values were below 0.2 for most fields. However, the K_c values varied from 0 to over 0.6 according to the level of residual surface moisture from winter, which is impacted by the previous crop and tillage history. The same impact is shown for the April and May images and for June 3, where effects of pre- or postplanting irrigation created a substantial range in K_c.

The NDVI and K_c show a strong relationship during the period from June 19 to September 15. During this period, fields having high NDVI values also had high K_c, because of the frequent irrigation coupled with high transpiration rates and reduced opportunity for evaporation from soil. On September 15, a wide range of K_c occurred in the fields having lower NDVI, because these fields were likely harvested and therefore ET from such fields depends only on residual surface moisture. Finally, in the fall (October 17), most fields returned to a bare soil condition, although there was still a large variation in K_c.

The limitation of K_c estimation by NDVI is more clear when a series of K_c versus NDVI relationships are overlaid. Fig. 7 shows K_c versus NDVI relationships for potato and sugar beet fields, for three satellite dates during the crop development period. For both crops, the K_c versus NDVI relationship appears as a similar triangular shaped cloud of points, with the minimum K_c increasing as NDVI increases. The bottom line of the triangle is indicated as a "basal K_c" in Fig. 7, and explains the contribution of crop transpiration in the total K_c. Any point above the "basal K_c" line reflects some contribution of soil evaporation, where the soil evaporation portion is independent of NDVI.

From these analysis results, it is clear that the estimation of ET for specific fields using a general crop coefficient curve or a NDVI-based K_c value is difficult, especially during periods of low vegetation cover. During these periods, an energy balance ET estimation model is a useful tool both for estimating the average ET of an area, and for estimating ET from individual fields. The K_c distributions during mid-season typically had smaller ranges with a more normal type of distribution. Therefore, estimating ET

from traditional "mean" K_c curves is relatively easier during midseason periods if applied general curves describe the average K_c for the area of interest. However, if one desires to estimate ET from individual fields using mean K_c curves, a range of ±0.1 variation in K_c values appears to exist even during the midseason. Therefore, even if the K_c curve perfectly describes the average values for the area of interest, a ±0.1 error in K_c is inevitable. The error range in predicted K_c would reduce significantly, especially during periods of low vegetation cover, if a dual K_c procedure that predicts the increase in K_c caused by a wet soil surface layer were utilized, for example those by Wright (1982) or Allen et al. (1998, 2005). These types of K_c estimates were not evaluated during this study due to the lack of knowledge of irrigation dates for individual fields.

Comparison of Mean K_c Curves from Energy Balance Model with Traditional K_c Curves

Averages of the K_c derived by the EB model for all classified fields are shown in Fig. 8 along with the general K_c curves of Allen and Brockway (1983) and AgriMet for year 2000 (AgriMet 2002b). The Allen and Brockway curves were developed for the Magic Valley area using K_c tables of Wright (1981), and have been expressed in terms of monthly averages. The curves have been used by the Idaho Department of Water Resources for evaluating water rights transfers and for planning studies and basin wide water balances. AgriMet curves by the U.S. Bureau of Reclamation (AgriMet 2002b) are a source of near-real time K_c and ET information frequently applied in this region. The basic curves for AgriMet are based on Wright (1981, 1995) and are typically adjusted each year using cropping dates based on surveys with University extension services and other contacts. Once the starting dates are determined for each crop, two other dates termed cover date and terminate date are estimated using historical data, and the basic curves are adjusted, timewise, based on the three "key" dates. The initially determined curves are occasionally adjusted during the cropping season by AgriMet based on reports by field experts (AgriMet 2002a).

The Allen and Brockway curves agreed relatively well with the EB-determined curves for sugar beet and grain crops, and agreed fairly well with those for alfalfa, where the K_c curve by Allen and Brockway was an averaged curve representing a mixture of cutting practices, and for potatoes, although the peak K_c for potatoes derived from the EB model averaged about 0.15 higher than that by Allen and Brockway. The curves from Allen and Brockway did not agree well for the three other crops (beans, corn, and peas). The good agreement between the satellite derived and Allen and Brockway K_c curves for three to five of eight crops is surprising when one considers that the Allen and Brockway curves represent long term averages developed in 1983 rather than specific curves for 2000 as derived from the EB model. The reasons for disagreement between curves for bean, corn, and pea fields are unknown, but it is possible that the popular varieties of crops or field management, including planting dates and plant spacing, might have changed since 1983.

The AgriMet K_c curves agreed well with the ET-determined K_c curves for alfalfa, bean, corn, potato, and sugar beet crops. Agreement was poor for pea and grain fields. Most differences between estimated and AgriMet general K_c curves may have been caused by nonrepresentative emergence and termination dates used by AgriMet for the particular crops in the Magic Valley area, and by more rapid growth rates and senescence rates predicted by AgriMet for peas and grain. In all situations, average peak K_c values by the EB model were equal to or greater than peak K_c values by AgriMet and Allen and Brockway, indicating that sampled Magic Valley fields did not suffer reduced ET as compared to the potential ET defined by the Wright (1981, 1995) K_c curves. This indicates good crop and water management practices in the region.

Use of Satellite Based Energy Balance Model to Refine Emergence, Cover, and Termination Dates for AgriMet Curves

Fig. 9 shows the average K_c curves by the EB model for the classified fields along with AgriMet K_c curves that were modified by adjusting the three "key" dates used in computing daily K_c values, namely the so-called start/cover/terminate dates of AgriMet (2002a). These dates were adjusted to make the AgriMet curves better fit the mean curves by the EB model. The adjustments were applied only to the three key dates, with the rest of the curve shape defined by the tabular values in AgriMet that express K_c as a function of percentage time from emergence to cover and from cover to termination. No adjustment was made to magnitudes of K_c values or curves. The adjusted key dates may more likely represent the general key dates for the study area for year 2000, if both the EB model derived and the basic AgriMet K_c curves are assumed to be reliable. Following the adjustment to key dates, the AgriMet curves almost perfectly fit the curves by the EB model for most crops, as shown in Fig. 9, with the exception of corn and spring grain.

Table 4 lists original AgriMet key dates for year 2000 and adjusted key dates. For alfalfa, the starting date was shifted to 12 days earlier. For bean and potato fields, AgriMet K_c values agreed well with the EB model derived values without any adjustment (see the Fig. 8), therefore impact of adjustment to key cropping dates was relatively small. The AgriMet K_c curve for corn did not agree well with the estimated curve, even though a large adjustment to key dates was applied. Corn and spring grain were the only crops where an adjusted AgriMet curve could not reproduce the curve derived by the EB model. A large adjustment was applied to dates for the AgriMet pea curve so that the adjusted cultivation period was much longer than originally. It indicates that the cultivation period predicted for the original AgriMet curve may have been too short. Peas are often used as a nurse crop for alfalfa, where alfalfa begins to grow following harvest of the peas. However, this combination was not observed in K_c from sampled pea fields, possibly due to limitations by the training set used during classifications.

The AgriMet curve for sugar beet crops agreed almost perfectly with the mean estimated curve, after adjustment to an earlier start and later harvest date. This might represent the actual field management practiced by farmers, as farmers tend to grow sugar beets longer in order to harvest beets having more sugar. Large adjustments were applied to grain fields. These large adjustments were required because the original AgriMet curves did not describe the slower reduction of K_c observed using the EB model during the late season. The rapid decrement of K_c in the original AgriMet curves leave some doubt, and the Allen and Blockway curve shown in Fig. 8 might have been more appropriate for this area.

In this analysis, the results from the EB model were used to refine the three key dates for AgriMet curves. Developing complete K_c curves using only EB model results might be a more straightforward and reliable way to obtain representative K_c curves for the study area. However, the development of curves must be done postseason or with at least a 1 month delay to

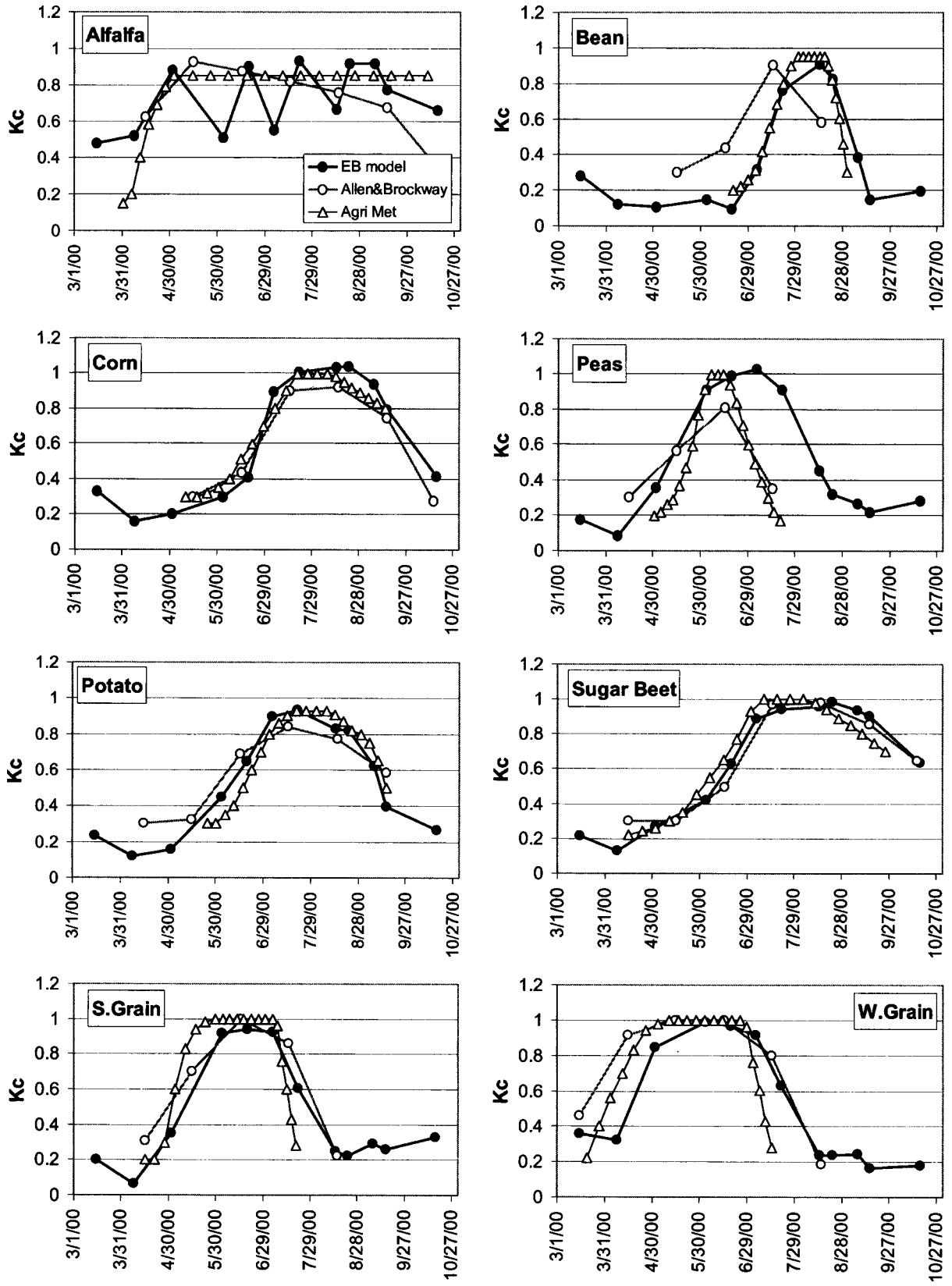

Fig. 8. Average K_c by satellite based energy balance model for all classified fields compared with general K_c curves for Twin Falls from Allen and Brockway (1983), and from AgriMet (2002b)

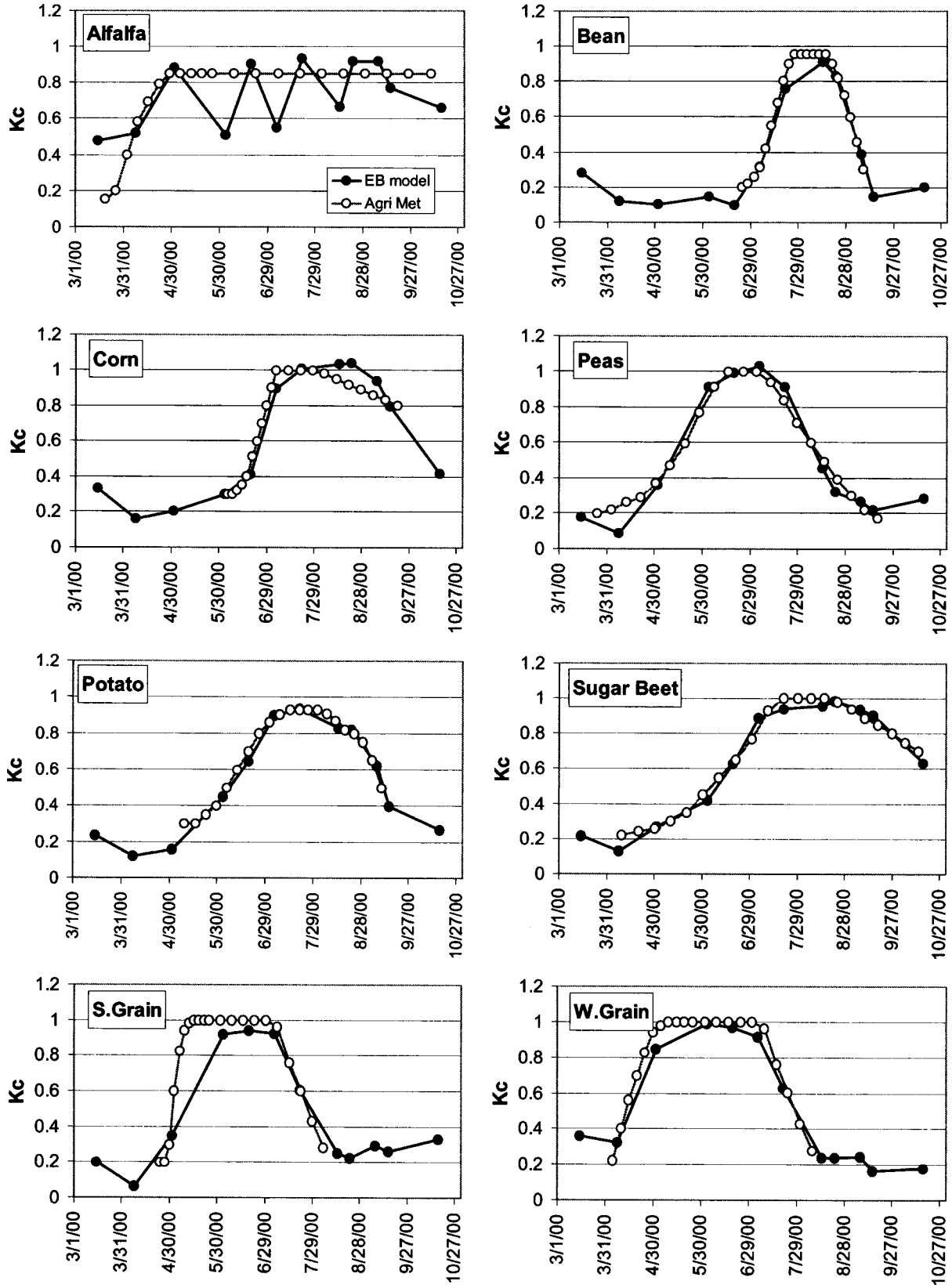

Fig. 9. Average K_c by satellite based energy balance model for classified fields compared with AgriMet K_c curves adjusted for three key dates

Table 4. Original and Adjusted Key Dates for AgriMet K_c Curves and Differences (Days)

Crop	Item	Start date	Cover date	Terminate date
Alfalfa	Original[a]	1 April	26 May	—
	Adjusted	20 March	26 May	—
	Difference[b]	−12	0	—
Bean	Original	20 June	4 August	30 August
	Adjusted	24 June	31 July	8 September
	Difference	4	−4	9
Corn	Original	10 May	20 July	14 September
	Adjusted	5 June	5 July	20 September
	Difference	26	−15	6
Pea	Original	1 May	10 June	20 July
	Adjusted	25 March	25 June	18 September
	Difference	−37	15	60
Potato	Original	25 May	20 July	15 September
	Adjusted	10 May	15 July	10 September
	Difference	−15	−5	−5
Sugar beet	Original	15 April	10 July	25 September
	Adjusted	10 April	21 July	14 October
	Difference	−5	11	19
Spring grain	Original	15 April	19 June	20 July
	Adjusted	24 April	25 May	5 August
	Difference	9	−25	16
Winter grain	Original	20 March	3 June	15 July
	Adjusted	5 April	25 May	8 August
	Difference	16	−9	24

[a]AgriMet does not issue original key dates from their web site. These original dates were analyzed using AgriMet crop evapotranspiration (ET) data and solving for key dates that reproduced the ET data. Therefore the dates shown might be incorrect by plus-minus 1 day from the actual values. The start date used by AgriMet represents the date of emergence.
[b]Negative differences indicate that the adjusted date is earlier than the original date.

provide for image processing time. Therefore combination of the traditional K_c curve or a curve derived from a previous year using the EB model with key dates determined by satellite might be a useful method for real-time field water management.

Applicability for Humid Regions

An interesting question was posed by a peer reviewer for this paper regarding the applicability of the presented techniques in humid regions where higher chances of cloudy dates are expected. This issue is discussed from two aspects; the first aspect regards problems caused by reductions in satellite image availability due to clouds, and the other aspect is the applicability of satellite-derived K_c curves to periods having cloudy conditions.

During the period of this study, two Landsat satellites (5 and 7) both having return periods of 16 days were available. This means that approximately four image dates per month were potentially available if conditions were clear. Landsat image paths have more than 30% overlap at 43° latitude, where the study area was located, so that more than 60% of the land mass resides within an "overlapping area" between adjacent paths. The overlapping area increases as latitude increases, and vice versa. If the area of interest happens to be in the "overlapped area" of two paths, image availability doubles, which means the potential availability of eight image dates (i.e., K_c values) per month using Landsat. Landsat 7 has been out of order since May 2003. Thus, currently, only four image dates per a month are potentially possible for path-overlapping areas.

Energy balance based ET estimation methods cannot be applied with cloudy satellite images. Therefore, the image availability is reduced in humid regions having clouds, and the reduction of image frequency affects the estimation accuracy of K_c or ET for integrated time periods. However, as long as clear-sky images are obtainable with a certain frequency (e.g., one image per month) during the crop cultivating period, one can successfully describe the actual K_c curves as presented in this paper, especially for crops having longer developing and full cover periods, such as corn, potato, sugar beets, and grain crops as shown in Figs. 4 and 5. Development of full K_c curves might be difficult if the availability of clear-sky images is less then once per month during the cultivating period. In such cases, the techniques followed in this paper might be used only as supplemental information, for example, to help determine any time shifting adjustment to traditional K_c curves or to determine actual K_c or ET distributions for only dates when clear sky images are available.

Once K_c values are established or calibrated using clear-sky satellite images, one applies this value to predict ET during intervening periods including those having cloudy days. However, there is some question whether K_c values determined under clear sky conditions apply to cloudy conditions, due to impact of clouds on stomatal responses and albedo. Figs. 1 and 10 show lysimeter observed K_c for sugar beet (1989) bean (1974), and corn (1976) crops at Kimberly, Id., along with calculated "basal" K_c curves based on Wright (1982) (Fig. 10 only). Some extreme high points in the K_c graphs are due to wetting events caused by either rainfall or irrigation. Cloudiness of each day is indicated by the ratio of measured solar radiation to the theoretical clear sky solar radiation (R_s/R_{so}). K_c values under clear sky conditions and cloudy conditions were similar, especially for sugar beets in 1989 (Fig. 1). A simple statistical analysis (F test at the 95% level of confidence) was applied to the bean and corn data shown in Fig. 10 to examine whether the magnitude of difference between observed total K_c and the basal K_c (K_c-K_{cb}) are affected by cloudiness. For the analysis, surface soil moisture was simply indicated by three levels; wet, moist, and dry, according to the days since precipitation/irrigation, as actual soil moisture measurements were not available. There was a slight statistically significant difference in K_c between clear and cloudy conditions for corn ($p = 0.05$). However, the overall analysis using the two crops together indicated that there was no statistical evidence that cloudiness (i.e., R_s/R_{so}) impacted K_c measured for any of the surface moisture levels. Therefore, we tentatively conclude that the K_c curves developed using clear sky satellite images are applicable to cloudy days in between satellite images, without any adjustment. Future study is recommended on this issue, through experiments designed to investigate this effect and using more crop types.

Summary and Conclusions

The actual distribution of K_c over many agricultural fields were investigated by crop type, using crop evapotranspiration derived from a satellite based EB model. K_c had a strong relation to NDVI during mid season periods. On the other hand, large ranges in K_c were observed during early and late growth periods when fields were in a nearly bare soil condition. For those field conditions and periods, the EB model is a useful tool for calculating K_c and ET for individual fields. The evaluation of two widely used sets of

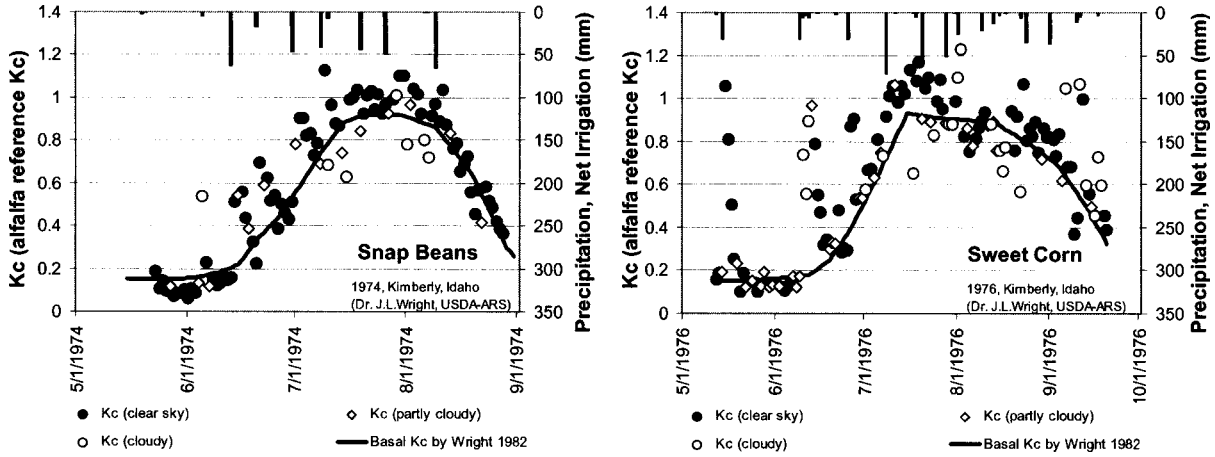

Fig. 10. K_c by lysimeter measured evapotranspiration in different cloud levels, for beans (1974) and corn (1976), unpublished lysimeter data from Wright (2000), USDA-ARS, Kimberly, Id. Cloud levels were defined by ratio of measured solar radiation to theoretical clear sky solar radiation (R_s/R_{so}) as: "clear sky:" $R_s/R_{so} \geq 0.85$; "partly cloudy:" $0.7 \leq R_s/R_{so} < 0.85$; "cloudy:" $R_s/R_{so} < 0.7$.

traditional K_c based ET curves in Idaho, one from Allen and Brockway (1983) and the other from the AgriMet internet based system (AgriMet 2002b), show that the traditional K_c curves represent the average field conditions relatively well for some crop types, but are quite different for crops where the variety or the actual field management may have changed since the traditional curves were developed. In the last part of this paper, the AgriMet K_c curves were adjusted according to K_c derived by the EB model by determining new values for the three "key" dates used to construct the crop curves. This simple adjustment worked very well in adjusting AgriMet curves to describe the general field conditions of the study area.

The satellite based energy balance model appears to be a useful method for evaluating the variation in populations of evapotranspiration and thus crop coefficient. This type of investigation provides some indication of the type of variation to be expected among fields of the same crop type. It is also useful for review of traditional crop curves and crop growth dates, or in developing "mean" K_c curves that represent the impact of surface wetting by rain and irrigation on the K_c curve. Further, one can use the technique, for example, to define the K_c curve for center pivot systems having high frequency irrigation. It is tentatively concluded through a statistical analysis for impact of cloudiness, that the presented techniques are applicable in humid regions also.

Considering that the mean K_c curves of Wright (1981, 1995) were fitted to lysimeter measurements representing high levels of water and agronomic management, and considering the relatively close agreement between the EB derived K_c curves and those of Wright during midseason for nearly 4,000 fields containing eight crops, it does not appear that ET for sampled crops in Magic Valley suffer from reduced ET caused by nonideal management or field conditions.

Acknowledgments

The writers acknowledge and thank Robin Wells and Chuck Coiner of Twin Falls for providing field identification information used to ground-truth the crop classification, the AgriMet system of the U.S. Bureau of Reclamation in Boise, Id. for providing valuable weather and crop information, Clarence Robison of the University of Idaho for assistance in statistical analyses and software support, and Dr. Wim Bastiaanssen of WaterWatch, the Netherlands, for guidance, review, and encouragement during University of Idaho research with the SEBAL and related models. The writers also thank the reviewers for thorough and useful comments that greatly improved the paper. This study was financially supported by a Synergy grant from NASA via Raytheon Company, the Idaho Dept. of Water Resources, and the University of Idaho.

References

AgriMet (2002a). "AgriMet crop coefficients." *U.S. Bureau of Reclamation, Pacific Northwest Region*, ⟨http://www.usbr.gov/pn/agrimet/cropcurves/crop_curves.htm⟩; (Sept. 17, 2003)

AgriMet (2002b). "The Pacific northwest cooperative Agricultural Weather Network." *U.S. Bureau of Reclamation, Pacific Northwest Region*, ⟨http://www.usbr.gov/pn/agrimet/⟩ (Sept. 17, 2003)

Allen, R. G. (1996). "Assessing integrity of weather data for reference evapotranspiration estimation." *J. Irrig. Drain. Eng.*, 122(2), 97–106.

Allen, R. G., and Brockway, C. E. (1983). "Estimating consumptive irrigation requirements for crops in Idaho." *Idaho Department of Water Resources*, ⟨http://www.kimberly.uidaho.edu/water/appndxet/index.shtml⟩ (Sept. 17, 2003).

Allen, R. G., Morse, A., and Tasumi, M. (2003). "Application of SEBAL for Western US water rights regulation and planning." *Proc. ICID Int. Workshop on Remote Sensing*, Montpellier, France.

Allen, R. G., Morse, A., Tasumi, M., Trezza, R., Bastiaanssen, W. G.M., Wright, J. L., and Kramber, W. (2002). "Evapotranspiration from a satellite-based surface energy balance for the Snake River Plain Aquifer in Idaho." *Proc., USCID/EWRI Conf. on Energy, Climate, Environment and Water*, San Luis Obispo, Calif.

Allen, R. G., Pereira, L. S., Raes, D., and Smith, M. (1998). "Crop evapotranspiration." *FAO Irrigation and Drainage Paper 56*, Food and Agricultural Organization of the United Nations, Rome.

Allen, R. G., Pereira, L. S., Smith, M., Raes, D., and Wright, J. L. (2005). "The FAO-56 dual crop coefficient method for predicting evaporation from soil and application extensions." *J. Irrig. Drain. Eng.*, 131(1), 2–13.

Bastiaanseen, W. G. M. (2000). "SEBAL-based sensible and latent heat fluxes in the irrigated Gediz Basin, Turkey." *J. Hydrol.*, 229, 87–100.

Bastiaanseen, W. G. M., and Bos, M. G. (1999). "Irrigation performance indicators based on remotely sensed data: a review of literature." *Irrig. Drain. Syst.*, 13, 291–311.

Bastiaanssen, W. G. M., Menenti, M., Feddes, R. A., and Holtslag, A. A. M. (1998a). "A remote sensing surface energy balance algorithm for land (SEBAL): 1. Formulation." *J. Hydrol.*, 212–213, 198–212.

Bastiaanssen, W. G. M., Noordman, E. J. M., Pelgrum, H., Davids, G., and Allen, R. G. (2005). "SEBAL model with remotely sensed data to improve water-resources management under actual field conditions." *J. Irrig. Drain. Eng.*, 131(1), 85–93.

Bastiaanssen, W. G. M., Pelgrum, H., Wang, J., Ma, Y., Moreno, J., Roerink, G. J., and van der Wal, T. (1998b). "A remote sensing surface energy balance algorithm for land (SEBAL): 2. validation." *J. Hydrol.*, 212–213, 213–229.

Bausch, W. C. (1993). "Soil background effects on reflectance-based crop coefficients for corn." *Remote Sens. Environ.*, 46, 213–222.

Bausch, W. C. (1995). "Remote sensing of crop coefficients for improving the irrigation scheduling of corn." *Agric. Water Manage.*, 27, 55–68.

Bausch, W. C., and Neale, C. M. U. (1989). "Spectral inputs improve corn crop coefficients and irrigation scheduling." *Trans. ASAE*, 32(6), 1901–1908.

Caselles, V., Artigao, M. M., Hurtado, E., Coll, C., and Brasa, A. (1998). "Mapping actual evapotranspiration by combining Landsat TM and NOAA-AVHRR images: Application to the Barrax area, Albacete, Spain." *Remote Sens. Environ.*, 63, 1–10.

Choudhury, B. J., Ahmed, N. U., Idso, S. B., Reginato, R. J., and Daughtry, C. S. T. (1994). "Relations between evaporation coefficients and vegetation indices studies by model simulations." *Remote Sens. Environ.*, 50, 1–17.

Doorenbos, J., and Pruitt, W. O. (1977). "Crop water requirements." *Irrigation and Drainage Paper No. 24*, Food and Agricultural Organization of the United Nations, Rome.

Environmental and Water Resources Institute of the ASCE Standardization of Reference Evapotranspiration Task Committee (EWRI). (2002). "The ASCE standardized reference evapotranspiration equation." ⟨http://www.kimberly.uidaho.edu/water/asceewri/⟩ (Sept. 17, 2003)

Hemakumara, H. M., Chandrapala, L., and Moene, A. F. (2003). "Evapotranspiration fluxes over mixed vegetation areas measured from large aperture scintillometer." *Agric. Water Manage.*, 58, 109–122.

Hunsaker, D. J., Pinter, P. J., Jr., Barnes, E. M., and Kimball, B. A. (2003). "Estimating cotton evapotranspiration crop coefficients with a multispectral vegetation index." *Irrig. Sci.*, 22(2), 95–104.

Jensen, M. E., ed. (1973). "Consumptive use of water and irrigation water requirements." Irrigation and Drainage Division, ASCE, New York.

Jensen, M. E., Burman, R. D., and Allen, R. G., (ed.). (1990). "Evapotranspiration and Irrigation water requirements." *ASCE Manual and Report* No. 70, ASCE, New York.

Kustas, W. P., and Norman, J. M. (1996). "Use of remote sensing for evapotranspiration monitoring over land surfaces." *Hydrol. Sci. J.*, 41(4), 495–516.

Moran, M. S., Jackson, R. D., Raymond, L. H., Gay, L. W., and Slater, P. N. (1989). "Mapping surface energy balance components by combining Landsat thematic mapper and ground-based meteorological data." *Remote Sens. Environ.*, 30, 77–87.

Morse, A., Allen, R. G., Tasumi, M., Kramber, W. J., Trezza, R., and Wright, J. L. (2001). "Application of the SEBAL methodology for estimating evapotranspiration and consumptive use of water through remote sensing." Idaho Department of Water Resources, Idaho.

Morse, A., Tasumi, M., Allen, R. G., and Kramber, W. J. (2000). "Application of the SEBAL methodology for estimating consumptive use of water and streamflow depletion in the Bear River Basin of Idaho through remote sensing." Idaho Dept. of Water Resources, Idaho.

Neale, C. M. U., Bausch, W. C., and Heerman, D. F. (1989). "Development of reflectance-based crop coefficients for corn." *Trans. ASAE*, 32(6): 1891–1899.

Nishida, K., Nemani, R. R., Glassy, J. M., and Running, S. W. (2003). "Development of an evapotranspiration index from Aqua/MODIS for monitoring surface moisture status." *IEEE Trans. Geosci. Remote Sens.*, GE-41(2), 493–501.

Norman, J. M., Kustas, W. P., and Humes, K. S. (1995). "Source approach for estimating soil and vegetation energy fluxes in observation of directional radiometric surface temperature." *Agric. Forest Meteorol.*, 77, 263–293.

Norman, J. M., Kustas, W. P., Prueger, J. H., and Diak, G. R. (2000). "Surface flux estimation using radiometric temperature: A dual-temperature-difference method to minimize measurement errors." *Water Resour. Res.*, 36(8), 2263–2274.

Romero, M. G., (2003). "Daily evapotranspiration estimation by means of evaporative fraction and reference evapotranspiration fraction." PhD dissertation, Utah State Univ., Logan, Utah.

Snyder, R. L., Lanini, B. J., Shaw, D. A., and Pruitt., W. O. (1989a). "Using reference evapotranspiration (ETo) and crop coefficients to estimate crop evapotranspiration (ETc) for agronomic crops, grasses, and vegetable crops." *Leaflet No. 21427*, Cooperative Extension, Univ. of California, Berkeley, Calif.

Snyder, R. L., Lanini, B. J., Shaw, D. A., and Pruitt, W. O. (1989b). "Using reference evapotranspiration (ETo) and crop coefficients to estimate crop evapotranspiration (ETc) for trees and vines." *Leaflet No. 21428*, Cooperative Extension, Univ. of California, Berkeley, Calif.

Tasumi, M. (2003). "Progress in operational estimation of regional evapotranspiration using satellite imagery." PhD dissertation, Univ. of Idaho, Moscow, Idaho.

Tasumi, M., Allen, R. G., and Bastiaanssen, W. G. M. (2000). "The theoretical basis of SEBAL." Idaho Dept. of Water Resources, Idaho, 46–69.

Tasumi, M., Trezza, R., Allen, R. G., and Wright, J. L. (2003). "US validation tests on the SEBAL model for evapotranspiration via satellite." *Proc., ICID Int. Workshop on Remote Sensing*, Montpellier, France.

Trezza, R. (2002). "Evapotranspiration using a satellite-based surface energy balance with standardized ground control." PhD dissertation, Utah State Univ., Logan, Utah.

Wright, J. L. (1981). "Crop coefficients for estimates of daily crop evapotranspiration." *Irrigation scheduling for water and energy conservation in the 80s*, ASAE, Dec. St. Joseph, Mich.

Wright, J. L. (1982). "New evapotranspiration crop coefficients." *J. Irrig. Drain. Div.*, 108(1), 57–74.

Wright, J. L. (1991). "Using weighing lysimeters to develop evapotranspiration crop coefficients." *Lysimeters for evapotranspiration and environmental measurements*, R. G. Allen, T. A. Howell, W. O. Pruitt, I. A. Walter, and M. E. Jensen, eds., ASCE, New York, 191–199.

Wright, J. L. (1995). "Calibrating an ET procedure and deriving ET crop coefficients." *Proc., Seminar on Evapotranspiration and Irrigation Efficiency*, American Consulting Engineers Council of Colorado and Colorado Division of Water Resources, Arvada, Colo.